CFD – STH Code Coupling for the Thermal Hydraulic Analysis of NACIE-UP Experimental Facility

P. Cioli Puviani, R. Zanino
NEMO Group, Dipartimento Energia
Politecnico di Torino
Corso Duca degli Abruzzi, 24, 10129 Torino, Italy
pietro.ciolipuviani@polito.it, roberto.zanino@polito.it

T. Del Moro, F. Giannetti
Department of Astronautical, Electrical and Energy Engineering DIAEE
Sapienza University of Rome
Corso Vittorio Emanuele II, 244, 00186 Rome, Italy
tommaso.delmoro@uniroma1.it, fabio.giannetti@uniroma1.it

B. Gonfiotti, I. Di Piazza, D. Martelli, M. Tarantino
ENEA, Department for Fusion and Technology for Nuclear Safety and Security C.R. Brasimone
40032, Camugnano (BO), Italy
bruno.gonfiotti@enea.it,ivan.dipiazza@enea.it,daniele.martelli@enea.it,
mariano.tarantino@enea.it

doi.org/10.13182/NURETH20-40088

ABSTRACT

GEN-IV Lead-cooled Fast Reactors are recognized as an economically competitive solution with intrinsic safe operation. ENEA is a member of the FALCON Consortium, which has the goal to construct the Advanced Lead-cooled Fast Reactor European Demonstrator (ALFRED) in the 2030s. In this framework, computational tools are required to support the design and safety assessment of new facilities and reactors. Computational Fluid Dynamic (CFD) codes are able to reproduce local phenomena (e. g., thermal stratification, fluid mixing and local distributions) by solving directly the three-dimensional Navier-Stokes equations, but at the price of high computational cost. Instead, System Thermal-Hydraulic (STH) codes solve one-dimensional equations and are more suited for system-scale analyses.
The goal of this work is to develop, validate and apply a simulation tool able to reproduce the TH behavior of Heavy Liquid Metals (HLMs) through the coupling between STH and CFD codes. The tool aims to exploit the advantages of the two families of codes and adopt a multi-scale approach for improved simulation at component level within system analysis, with an acceptable computational time. The coupling technique is based on FORTRAN user routines implemented in Ansys CFX, i.e. the master CFD code,. The STH code used in this activity is RELAP5/MOD3.3. The user routines take care of data exchange, RELAP5 execution, and error checking. The coupled simulation tool is adopted to reproduce experimental data on a forced-to-natural-circulation transition test, carried out on the NACIE-UP facility, with LBE as working fluid. Limitations of the present analysis and plans for future improvements will be discussed.

KEYWORDS
Coupling, CFD, STH, HLM, NACIE

1. INTRODUCTION

The need for sustainable and safe energy sources requires the development of innovative technologies. In the nuclear field, the research sees GEN IV reactors as one of the answers for economically competitive solutions with intrinsic safe operation: among them, Lead-cooled Fast Reactors (LFRs) are considered as one of the most promising designs [1]. ENEA and the partners of the FALCON consortium are carrying on an R&D program for ALFRED, the 300 MWth pool-type European LFR demonstrator. The program is mainly based on experimental facilities devoted to the testing and improvement of the design of ALFRED components and to increase the Technology Readiness Level (TRL) of the proposed solutions [2].

Computational tools are required to support the design and safety assessment of pool-type experimental facilities. CFD codes, as Ansys CFX, and System Thermal-Hydraulic (STH) codes, as RELAP5, are currently adopted for thermal-hydraulic (TH) analyses. The goal of this work is to develop, apply and validate a simulation tool able to reproduce the TH behavior of Heavy Liquid Metals (HLMs) through the coupling between STH and CFD codes. The tool will exploit the advantages of the two families of codes and will adopt a multiscale approach for improved component simulation within system analysis [3].

During the past decade, a coupled approach has been implemented with different codes [4], adopting various STH codes as RELAP5, ATHLET, TRACE, and CFD codes as Fluent, Ansys CFX, STAR-CCM+, with application to both GEN-III and GEN-IV technologies. Examples of previous works on the topic are reported in [5, 6, 7, 8, 9].

In this work, the STH code RELAP5/Mod3.3 has been coupled with the Ansys CFX commercial code, through a novel approach that adopts in-house developed tools for the data post processing and exchange, completely managed by the Ansys CFX code. The work presented in this paper is the first step towards the validation of the coupling architecture against an experiment performed in the NACIE-UP facility, located at the ENEA Brasimone Research Center. A coupled tool has already been developed and applied to the NACIE-UP facility [10] but in that case Ansys Fluent was used as the CFD code. The tool is written in Python and Fortran.

The first validation exercise of the tool is realized through the post-test analysis of experimental data released in the framework of the IAEA international benchmark CRP I31038 “Benchmark on Transition from Forced to Natural Circulation Experiment with Heavy Liquid Metal Loop”. The application of this coupled tool intends to increase the maturity and confidence in adopting CFD-STH coupling, to support the design, transient analysis, and safety assessment of LFR.

2. NACIE-UP FACILITY

2.1. NACIE-UP Facility Description

NACIE-UP [11] is a Lead-Bismuth Eutectic (LBE) cooled rectangular loop with an overall height of 7.7 m. It is composed by an electrical Fuel Pin Bundle Simulator (FPBS) in the bottom left part, an expansion vessel at the top left, and a double wall tubes Heat Exchanger (HX) at the top right with the gap between the LBE and the water (secondary coolant) filled with AISI 316L powder and pressurized air. LBE is moved by gas lift. A schematic drawing of the facility is shown in Figure 1. The facility is equipped with several thermocouples monitoring the temperatures of the loop, with focus on the FPBS. The mass flow rate is measured by a prototypical Thermal mass Flow Meter (TFM) developed in ENEA in collaboration with

Thermocoax, which is based on the energy balance between the power delivered by the instrument to the fluid and the temperature variation across the electrical heater.

The FPBS is composed of 19 wire-spaced electrical rods, arranged in a triangular lattice with a pitch-to diameter ratio of about 1.28. The pin diameter is equal to 6.55 mm, while the wire diameter is 1.75 mm and it is helicoidally twisted around the pin with an helical pitch of 262 mm. Each pin is 2000 mm long with an active length of 600 mm. In the "pre-active" length about ~8-10% of the overall power is provided to the fluid. The pins are kept in position by a grid downstream the FPBS. The bundle is contained in a hexagonal wrapper. The drawing is reported in Figure 2. Instrumentation in the FPBS is located on Plane 1, Plane 2 and Plane 3, respectively at 38, 300 and 532 mm from the beginning of the active length, and on the Pin3 wall every 43.7 mm after the Plane 1 [11].

The expansion vessel must accommodate the thermal expansions of the LBE and keeps the cover gas pressure at the required set point. It is equipped with two level sensors that fix the LBE level during the filling of the facility.

The HX is a shell and tube type, composed of 7 double wall tubes, with the LBE flowing tube side from the top to the bottom of the component. There are two parts composing the shell side: a "low power section" (0-30 kW), where the secondary fluid moves in cross flow with respect to the LBE, and a "high power section" (30-250 kW), where the water flows shell side in counter-current with respect to the LBE. The secondary side is a closed loop working with pressurized water at 16 bar, equipped with a circulation pump, a pressurizer, and an air cooler. In the experiment considered for the benchmark, only the "high power section" of the HX has been used to facilitate the numerical modelling of the facility. The double wall of the HX is filled with stainless steel powder and pressurized air, with the thermal conductivity that can be evaluated through the following formula [12]:

$$k_{powder} = 0.3 + 0.005 \cdot (T - 200) \quad (1)$$

where T is in °C and k is in W/(m·K).

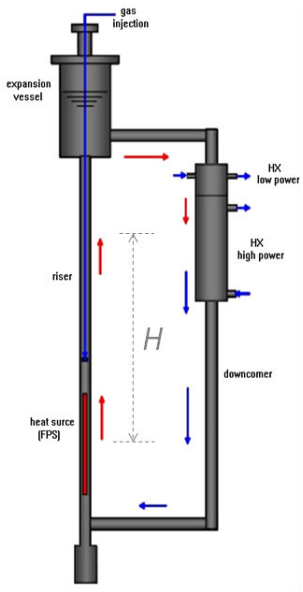

Figure 1. Schematic drawing of the NACIE-UP primary loop

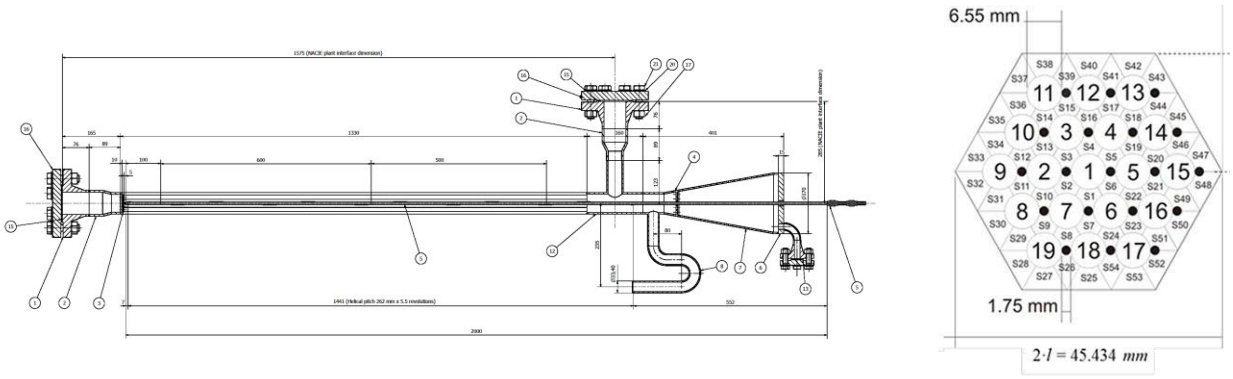

Figure 2. NACIE-UP FPBS layout (left) and cross section view (right)

2.2. Description of the ADP10 Experimental Test

The experimental test (named ADP10) analyzes the transition between an initial steady state in forced circulation, when the fluid flow is enhanced by the gas injection in the riser line, to a second steady state during which natural circulation is established. The transition starts when the gas injection is stopped leading to a sudden reduction of the LBE mass flow rate, therefore the natural circulation is the only mean to drive the LBE flow. Since the FPBS power (uniformly distributed among the 19 pins) remains constant during all the test, the LBE temperature downstream the FPBS increases, whereas the upstream one decreases.

In the first steady state, the gas is injected at a constant flow rate of 10 Nl/min. Water in the secondary side is kept at 16 bar, with a constant temperature at the HX inlet of 170°C, and the volumetric flow rate is 10 m^3/h. At t=0, the gas flow rate drops to zero in 1 s, while all the other parameters remain constant. After the transition, a new steady state condition is achieved, and it is kept for more than 30 minutes.

The CFD stand-alone model is adopted for the analysis of the two steady states while the STH and coupled simulation reproduce the entire transient. In the following, the CFD results are presented only for the first steady state, since the scope of the paper is to present the coupled tool results.

3. NACIE-UP NUMERICAL MODELS

3.1. ANSYS CFX Simulation

3.1.1. Description of the CFD numerical model

The CFD domain is limited to the 600 mm of the active region of the FPBS because of the high computational cost of the simulation. The simulated domain comprehends the LBE [13] fluid region, the external solid wrapper, the wires and the external 1 mm of the pins, all considered as AISI 316L [11].To limit the number of nodes, the mesh has been decomposed in different bodies both axially and radially, to achieve a structured mesh on each region. The cost of this operation is the high number of interfaces, which also limits the number of partitions in which the coupled simulation could be run to keep under control the time needed for interface interpolation.

At the FPBS inlet, a fully developed velocity distribution is imposed. The selected turbulence model is the $SST\ k-\omega$ [15] with a constant Pr_t of 1.5 (from a sensitivity, negligible differences are found in the range 1.5 – 2). On the external wall of the solid structure, an adiabatic condition is imposed. The fluid boundary layer at the wall is resolved with a $y^+ \sim 1$.

A grid independence study (Table I) has been carried out to evaluate the number of nodes that represents a compromise between accuracy and computational time consumption. The *Coarse improved* mesh (Figure 3) of 4.5 M of nodes starts from the Reference one, varying the element the near wall treatment and the element size that control the mesh in the radial direction and post-producing the mesh merging closed nodes between different bodies. This mesh (shown in Figure 3) has been selected due to the need of reducing as much as possible the mesh dimension, reaching discrepancies lower than 10%, value in the range of typical error of the turbulence model.

Table I. Grid independence study of the FPBS CFD model

	Coarse	Coarse improved	Reference	Radial ref	Axial ref
n° of nodes [M]	4.2	4.5	6.4	33.5	29.3
Δp [mbar]	28.4	31.1	31.4	33.6	33.8
ΔT in-out [°C]	80.1	80.3	80.3	80.3	80.4
T point [°C]	319.0	321.2	322.5	323.1	323.7

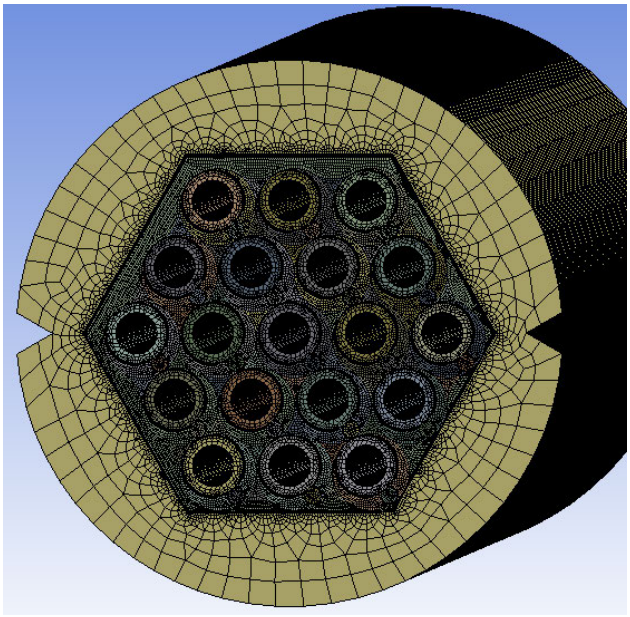

Figure 3. Coarse improved mesh

Table II. CFD steady state boundary condition [11]

Steady state			
Parameter	**Data**	**σ**	**σ[%]**
$\dot{m}_{LBE}$ [kg/s]	2.56	0.28	11
Q_act [W]	27000	1053	3.9
$T_{in,FPS}$[°C]	231.3	1.5	0.6%

3.1.2. Steady state results

The comparison between CFD and experimental data of the initial steady state in forced circulation concerns the surface averaged temperature variation through the heating region of the FPBS that is well reproduced by the code, and the local temperature in 67 Thermo-Couples (TCs) position. The experimental boundary conditions are reported in Table II, where σ indicates the uncertainty of the measurement instrument.

Only the results of some TCs in each of the three instrumented planes are reported from Figure 4 to Figure 6, and the axial variation on the wall embedded TC of Pin 3 in Figure 7.

The temperatures errors exceed the value of 1 °C intrinsic in the TCs measurement. While the values in planes 1 and 2 are of the same order of magnitude, the ones in the third plane are more than 2 times higher. The highlighted difference between CFD and experimental data is visible also in Figure 7, where the expected linear trend of the temperature of the TC of Pin 3 is represented by the code, while around 450 mm from the start of the active length the experimental values slightly flex. Possible reason for this behavior could be found in a non-uniform heat production in the pins at the end of the active length, which could explain the deviation from the linear trend visible on the last points of Figure 7.

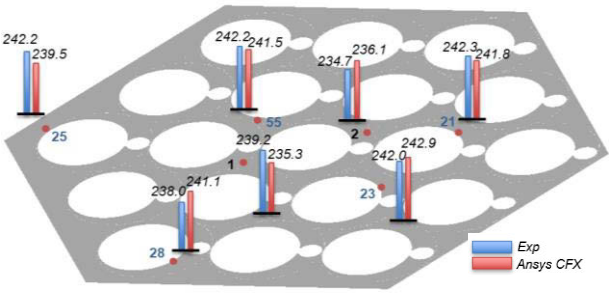

Figure 4. TCs temperature comparison on Plane 1

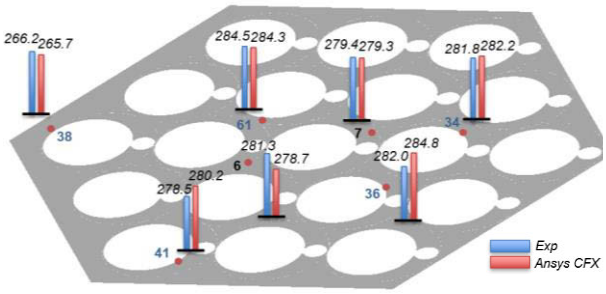

Figure 5. TCs temperature comparison on Plane 2

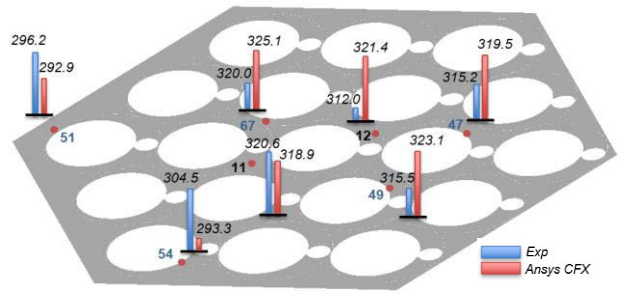

Figure 6. TCs temperature comparison on Plane 3

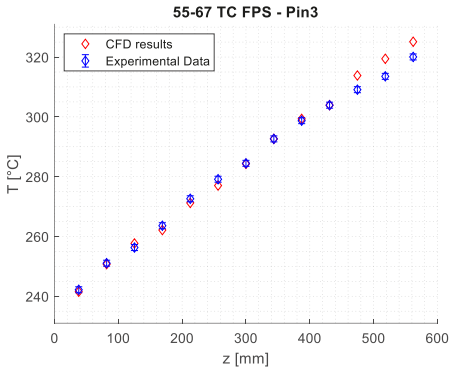

Figure 7. Pin 3 wall embedded temperature comparison

Table III. Mean and maximum temperature difference between CFD and experiment

Difference between experimental and CFD	Bulk TC		Wall TC	
	Mean	**Max**	**Mean**	**Max**
Plane 1	2.2 °C	4.0 °C	1.6 °C	3.0 °C
Plane 2	1.3 °C	2.6 °C	1.5 °C	3.2 °C
Plane 3	5.6 °C	9.4 °C	6.3 °C	11.4 °C

3.2. RELAP5 Simulation

3.2.1. Description of the RELAP5 numerical model

A model of NACIE-UP facility has been realized through the RELAP5/Mod3.3 code, properly modified to implement the HLMs thermo-physical properties. The model is constituted by PIPE components that model the fluid region, connected by SINGLE JUNCTION components, while the solid parts are modelled through heat structures. The mesh size spans between 5 cm in the active regions, and a maximum value of 12 cm in the non-active ones, with a smooth transition between the minimum and the maximum values. The nodalization is reported in Figure 13 (left).

Since RELAP5 allows the user to insert Reynolds-dependent friction and form losses coefficients, different correlations have been used in the components. For the localized pressure drops, formulas have been taken from Ref. [16], while for the FPBS the Cheng and Todreas correlation for wire-wrapped tube bundles [17-18] have been used. RELAP5 allows the friction factor to be inversely proportional to Re in the laminar region, while an exponential relation might be selected in the turbulent region. In the transition region, identified by RELAP5 in the Re range between 2200 and 3000, the friction factor in the result of a linear interpolation between the two regions [19]. Therefore, the actual correlation has been approximated by the following equations in the Re range of interest, with the calibration coefficients reported in Table IV, and the graphical comparison is shown in Figure 8.

$$\begin{cases} f_L = \frac{64}{\Phi_S \cdot Re} & if\ Re < 2200 \\ f_{L,T} = \left(3.75 - \frac{8250}{Re}\right)\left(f_{T,3000} - f_{L,2200}\right) + f_{L,2200} & if\ 2200 < Re < 3000 \\ f_T = A + B \cdot Re^{-C} & if\ Re > 3000 \end{cases} \quad (2)$$

Table IV. Coefficients for the calibration of the FPBS pressure drops in the RELAP5 model

Constant	Φ_S	A	B	C
Value	0.45	0.021	31.66	0.856

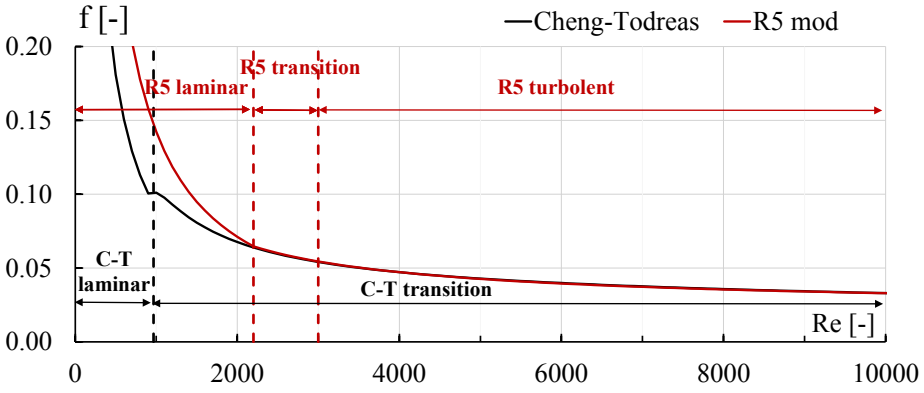

Figure 8. Cheng and Todreas vs RELAP5 correlations for wire wrapped tube bundles

3.2.2. Results

The steady state has been achieved through a 5000 s of transient simulation with constant boundary conditions. The boundary conditions are reported in Table V. The boundary conditions for the heat loss calculation have been set to 8 W/(m^{2}K) and 10°C as wall heat transfer coefficient and room temperature, respectively.

Table V. Boundary condition for ADP10 test

Parameter	Unit	Value
Gas mass flow rate	Nl/min	10
Water mass flow rate	m^3/h	10
Water inlet temperature in the HX	°C	170
Power provided in the active zone	W	27000
Power provided in the non-active zone	W	2236
Power provided by the TFM	W	1915

The instant in which the argon injection is stopped is the Start of the Transient (SoT) and it is assumed to be at t=0 s. The thermal power provided by the FPBS remains constant, as well as the water temperature and mass flow rate. As shown in Figure 9, the LBE mass flow rate rapidly drops at ~1 kg/s as soon as the gas injection is stopped, and after ~1500 s, a new steady state establishes after the transition to the natural circulation regime. Despite Reynolds-dependent pressure drops coefficients have been inserted in the numerical model, the mass flow is higher compared to the experiment in the second steady state, while in the first one the quantities show very good agreement. The discrepancies could be reconducted to errors in reproducing pressure drops at low Re. Another source of uncertainty can be addressed to the powder conductivity in the HX double wall tubes, which can impact on the temperature, and thus on the density of the downcomer, affecting the natural circulation.

Figure 10 shows that the FPBS inlet temperature is well predicted by the code, as well as the HX outlet temperature. Due to the higher mass flow rate predicted by the code, the temperature difference across the components is lower compared to the experimental one. In fact, the LBE temperature at the FPBS outlet (and HX inlet) is lower than the experimental value. The comparison of the RELAP5 results with the experimental data has been performed only with the integral values since local temperatures in the FPBS cannot be well predicted by STH codes.

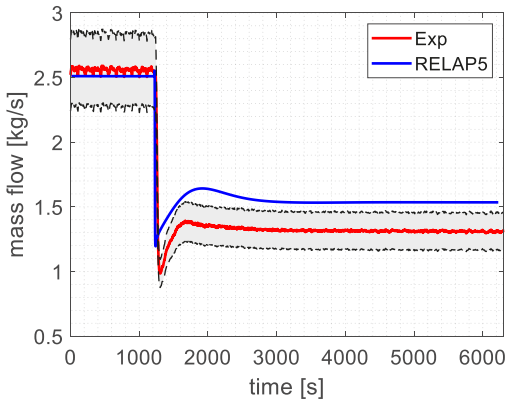

Figure 9. Exp vs R5 LBE mass flow rate

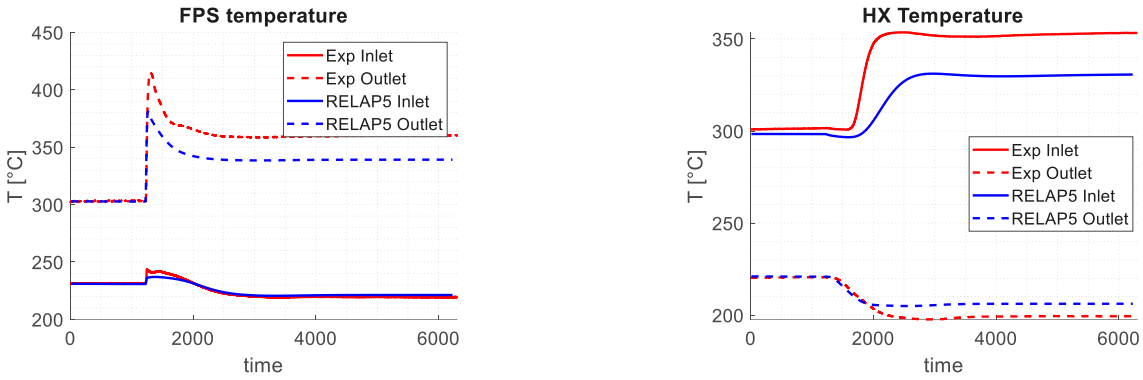

Figure 10. Exp vs R5 LBE temperatures at FPBS (left) and HX (right) inlet and outlet

3.3. ANSYS CFX – RELAP5 Simulation

3.3.1. Coupling Tool Description

The coupling between ANSYS CFX and RELAP5 has been realized through FORTRAN77 routines that are called in specific "time-locations" of the ANSYS CFX run, which is the master of the coupling process. These routines must guarantee the synchronization between the codes during the coupled simulation execution and the data exchange. The coupling strategy is based on a two-way connection, with partitioned and sequential solution. The time advancing scheme adopted is explicit (Figure 11) and the spatial domain approach is non-overlapping. Other details are reported in Table VI, in which the classification follows the guidelines of Ref. [4].

Table VI. Coupled methods classification

Code Integration	Partitioned Solutions
Coupling Execution	In-line approach
Synchronization	Sub-cycling approach
Information Exchange Type	Sequential coupling
Spatial Domains	Non-overlapping domain
Numerical Scheme	Explicit

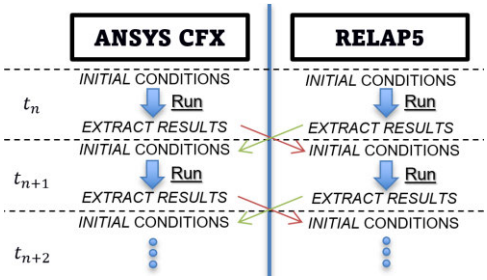

Figure 11. Explicit numerical scheme

The routines are divided in one User CEL (CFX Expression Language) Function and three Junction box routines, the latter are briefly described in the following:

- *jbr_userinput*: called before the start of the first timestep, this routine read from a *.dat* file the data needed to run the coupling, in particular the file name and path, the number and the name of Ansys CFX variable to be passed to RELAP5 and vice versa;
- *jbr_userinput_sott*: called after the start of the each timestep, this routine read the RELAP5 variable to be passed to Ansys CFX;
- *jbr_endofthetimestep*: called at the end of the each timestep, this routine modifies the RELAP5 input file inserting the results of the Ansys CFX timestep, run the RELAP5 timestep and process the created *.rst* file to extract the variable to be passed to Ansys CFX in a *.dat* file, append the last result to a *.plt* file and reduce the dimension of the *.rst* to avoid the manipulation of big files.

The User CEL Function, called *set_cfx_bc*, sets the boundary condition of the Ansys CFX timestep stored in the memory during the *jbr_userinput_sott* routine and is called autonomously by the code. The routines take advantage of in-house developed executable, written in python, for the RELAP5 input modification and post processing.
Eventually the results are collected in the Ansys CFX file in the *.trn* format and in the *.plt* file for what concerns the RELAP5 domain.
In Figure 12 a schematic of the code diagram is reported.

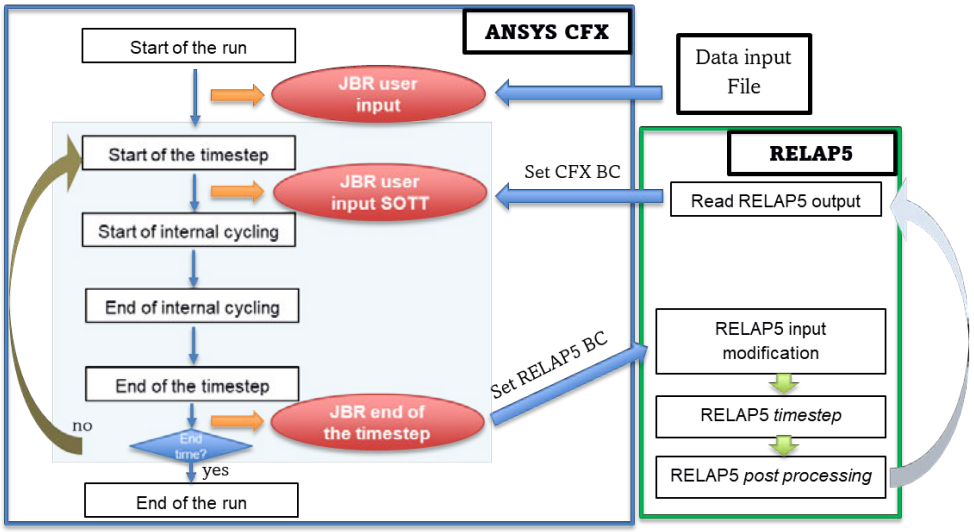

Figure 12. Coupling Scheme between Ansys CFX and RELAP5

3.3.2. Description of the Numerical Model and the Coupled Simulation Set Up

For the coupled simulation, the RELAP5 model has been modified removing the active part of the FPBS and inserting time dependent volumes (TMDPVOL) and time dependent junctions (TMDPJUN), where the boundary conditions from the CFD calculation are imposed. A preliminary RELAP5 steady state calculation with the "open loop" model has been performed to prepare a restart file to be used for the coupled simulation. The steady state values of the boundary conditions adopted for the "open loop" are those obtained with the entire loop.

During the coupled run the two-way exchange of information regards:

- the outlet mass flow rate, the outlet temperature and the pressure drop inside the active length of the FPBS, that are passed by Ansys CFX to RELAP5 through the TMDPJUN 261, the TMDPVOL 260, and the TMDPVOL 250, respectively;
- the inlet mass flow rate and the inlet temperature in the FPBS from RELAP5 to CFX, to be imposed at the inlet of the CFD model.

The pressure imposed at the TMDPVOL is calculated by the sum of three contributions:

- the CFD pressure drop;
- the pressure head;
- the pressure of the RELAP5 control volume 105 at the previous timestep, which center corresponds to the outlet of the CFD domain.

This calculation allows to set the relative pressure to zero at the outlet of the CFD model, with an impact in reducing the momentum equation residuals.

The CFD inlet mass flow rate corresponds to the RELAP5 value at the outlet of the "open loop" by applying a velocity map correspondent to a fully developed flow.

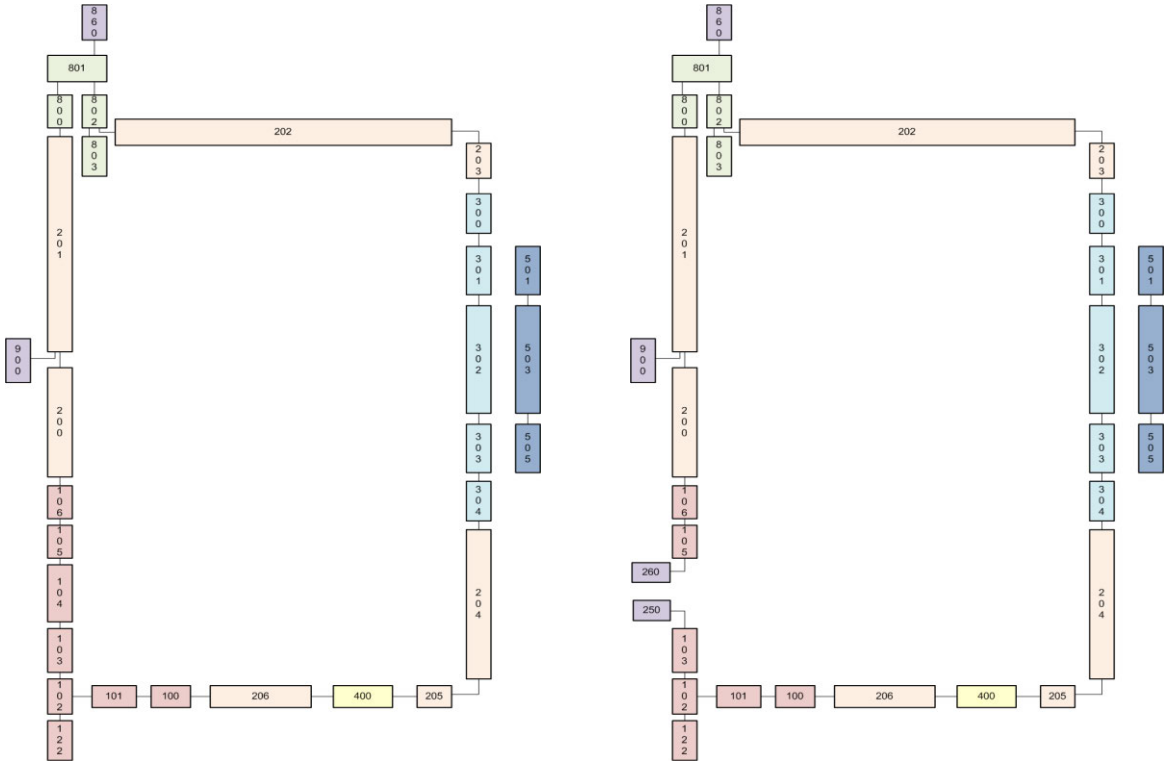

Figure 13. Nodalization of the NACIE-UP loop: closed loop (on the left) and open loop (on the right)

3.3.2 Results

The simulations have been carried out varying the timestep from 1e-3 s to 2e-2 s for Ansys CFX and, in turn, for the exchange of information; the RELAP5 code always runs with 1/10 of the coupling timestep, to improve stability of the STH code.

After 10 s coupled simulation, a steady state conditions establishes after the start of the variable exchange between codes. At this moment, the gas injection is stopped and the transient is triggered. All the cases with different time steps exhibit an oscillating behavior of the mass flow and pressure between 5 and 15 s. To verify the impact of the CFD model on the stability, the same simulations have been carried out with a hexagonal porous media, instead of the fluid and solid regions, maintaining the external wrapper. The pressure drops curve of the porous media has been calibrated with the RELAP5 correlations. It has been found out that also in this case the oscillations persist. Other runs with the CFD detailed model have been performed (i) changing the reverse flow coefficients in the RELAP5 junctions to dump eventual pressure waves, (ii) avoiding CFX to pass the mass flow rate value to RELAP5, but the results are characterized by the same oscillating behavior. Except for a single case, adopting the CFD detailed model, the oscillations diverge bringing to the failure of the simulations.

In Figure 14 and Figure 15 the experimental data are compared with the results obtained with the RELAP5 stand-alone run and coupled simulations with both the porous and full geometry CFD models. It is shown that the results of the coupled simulations almost overlap the RELAP5 stand-alone results. In the analyzed time frame, the coupled simulation does not show significant improvements in reproducing the experimental test, meaning that the RELAP5 and CFX results do not strongly differ and that the discrepancies with the experimental data can be addressed to the modelling of the FPBS. This consideration is strengthened by Figure 16, where it is showed that negligible discrepancies in reproducing the pressure variation in the FPBS between CFX and RELAP5.

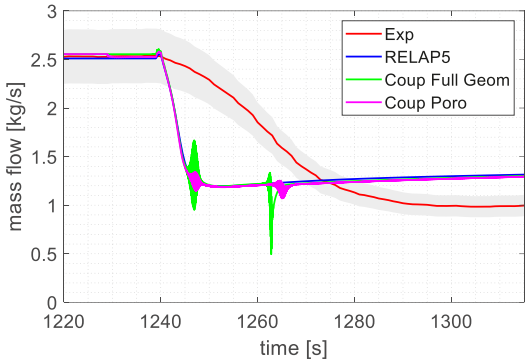

Figure 14. Code to code to experiment mass flow rate comparison

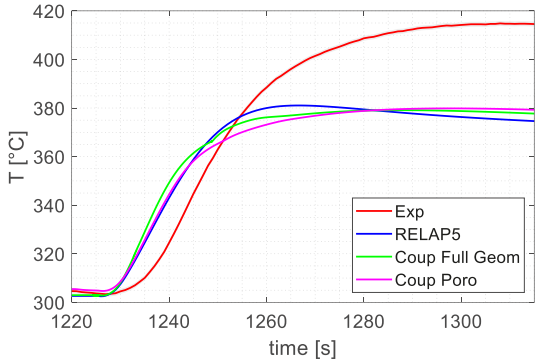

Figure 15. Code to code to experiment FPBS outlet temperature comparison

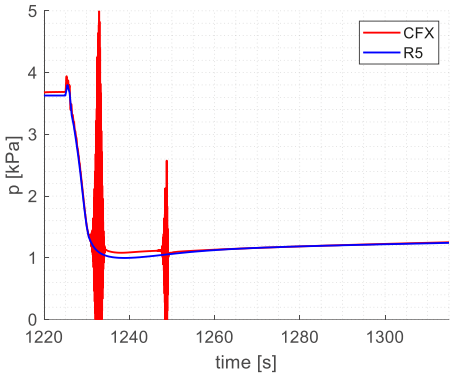

Figure 16. Code to code FPBS static pressure drop comparison

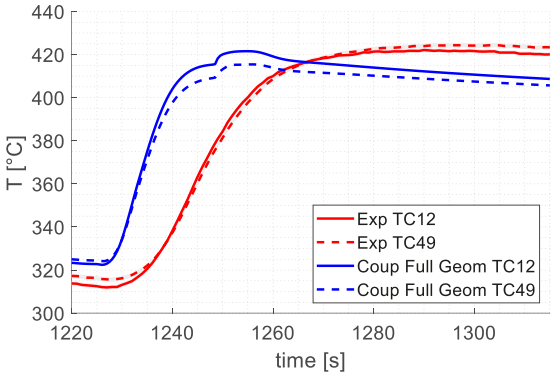

Figure 17. Coupled tool to experiment TC12 and TC49 temperature comparison

On the other hand, with the coupled simulation it is possible to compare the temperature variation in the TCs location in time with appropriate boundary conditions.
Also, for the local temperature results the behavior is similar to the one showed for the FPBS outlet temperature, whereas a change in the derivative could be noticed when the second mass flow rate oscillation is stabilized (Figure 17). The discrepancies between the mass flow rate affect the CFD values with respect to the experimental temperatures.

Since the stability problems affect the reliability of tool, the detailed geometry coupled simulation has been investigated also removing the non-condensable gas from the RELAP5 model to avoid sources of instability in the simulation, since it is an issue of the current version of the RELAP5/Mod3.3 code, although being the only one available that allows the use of the non-condensable gases. The model of the expansion vessel

has been redefined to include only the liquid volume, assuming no relevant variation in the LBE free level. As momentum source of the loop, a time-dependent junction fixes the LBE mass flow rate and becomes a single junction at the beginning of the coupled simulation.

The results show the absence of the oscillating behavior of the variables, with a faster decrease of the mass flow rate due to the instantaneous loss of the momentum source and the absence of the inertia due to presence of the gas in the first seconds after the stop of its injection (Figure 18). In turn, the temperature transition in the system is affected with a faster rise and a lower temperature peak (Figure 19).

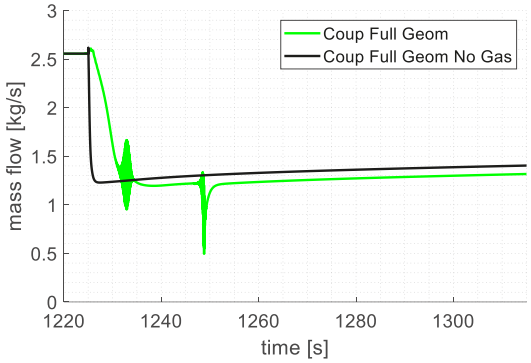

Figure 18. Coupled tool mass flow rate w/ and w/o gas injection

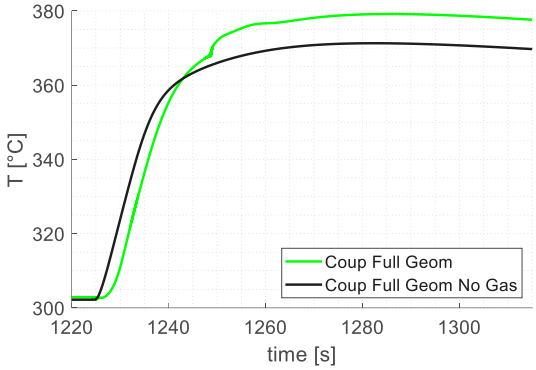

Figure 19. Coupled tool FPBS outlet temperature w/ and w/o gas injection

4. CONCLUSIONS AND PERSPECTIVE

The paper presents the first validation exercise of a CFD-STH coupled tool applied to the LBE-cooled loop facility NACIE-UP. The tool is described together with the stand-alone models of the RELAP5 and Ansys CFX codes. The CFD steady state stand-alone results show errors in representing the local bundle temperature of around 2°C on the instrumented Plane 1 and 2 (at 38 and 300 mm from the start of the active length), while the discrepancies increase in the Plane 3 (562 mm). RELAP5 integral parameters (i.e., temperatures) and mass flow rate agree with the experimental data during the initial steady state, while discrepancies can be found during the transition to the natural circulation and in the second steady state.

The coupled tool results show instabilities independent from most of the simulation parameters, but that could be prevented by avoiding the simulation of the non-condensable gases in the STH code. The obtained mass flow rate and averaged temperatures are in agreement with the RELAP5 stand-alone results, with small discrepancies in the time-frame investigated. The tool gives a local temperature description in the FPBS active length, although the results are mostly affected by the error in the mass flow rate calculation.

Further development of the two stand-alone models will help to reduce the differences with the experimental data, looking for a better representation of pressure drops and heat losses. A new semi-implicit time advancing scheme will be developed, which is expected to favor the stability of the coupled simulation and give the possibility to enlarge the timestep and in turn, the timeframe of the simulation to see the effect of the CFD FPBS model on the natural circulation condition at the end of the transient.

REFERENCES

1. P. Lorusso, S. Bassini, A, Del Nevo, I. Di Piazza, F. Giannetti, M. Tarantino, M. Utili, “GEN-IV LFR development: Status & perspectives”, *Prog. Nucl. Energy*, 105, 318-331 (2018). https://doi.org/10.1016/j.pnucene.2018.02.005

2. M. Tarantino, S. Bassini, D. Rozzia, "ALFRED PROJECT Research and Development Needs", ENEA Report ID: LR-P-R-126, CR Brasimone, March 2015
3. V. Moreau, M. Profir, A. Alemberti, M. Frignani, F. Merli, M. Belka, O. Frybort,T. Melichar, M. Tarantino, S. Franke, S. Eckert, A. Class, J. Yanez, D. Grishchenko, M. Jeltsov, P. Kudinov, F. Roelofs, K. Zwijsen, D.C. Visser, A. Badillo, B. Niceno, D. Martelli, "Pool CFD modelling: Lessons from the sesame project", *Nucl. Eng. Des.*, **355**, 110343 (2019) https://doi.org/10.1016/j.nucengdes.2019.110343
4. A. Pucciarelli, "Coupled system thermal Hydraulics/CFD models: General guidelines and applications to heavy liquid metals", *Ann. Nucl. Energy* (2020)
5. D. L. Aumiller, E. T. Tomlinson, R. C. Bauer, "A coupled RELAP5-3D/CFD methodology with a proof-of-principle calculation", *Nucl. Eng. Des*, 205, 83-90 (2001). https://doi.org/10.1016/S0029-5493(00)00370-8
6. D. Bertolotto, A. Manera, S. Frey, H.-M. Prasser, R. Chawla, "Single-phase mixing studies by means of a directly coupled CFD/system-code tool", *Ann. Nucl. Energy* (2009)
7. W. Li, X. Wu, D. Zhang, G. Su, W. Tian, S. Qiu, "Preliminary study of coupling CFD code FLUENT and system code RELAP5", *Ann. Nucl. Energy* (2014)
8. T. P. Grunloh, and A. Manera. "A novel domain overlapping strategy for the multiscale coupling of CFD with 1D system codes with applications to transient flows" *Annals of Nuclear Energy* (2016)
9. N. Forgione, M. Angelucci, C. Ulissi, D. Martelli, G. Barone, R. Ciolini and M. Tarantino, "Application of RELAP5/Mod3.3 – Fluent coupling codes to CIRCE-HERO, *Journal of Physics: Conference Series*, 1224 (2019). DOI: 10.1088/1742-6596/1224/1/012032
10. D. Martelli, N. Forgione, G. Barone and I. Di Piazza, "Coupled simulations of the NACIE facility using RELAP5 and ANSYS FLUENT codes", *Annals of Nuclear Energy*,101, 408-418 (2017).
11. I. Di Piazza, H. Hassan, P. Lorusso, D. Martelli, "Benchmark Specifications For Nacie-Up Facility: Non-Uniform Power Distribution Tests", ENEA Report ID: NA-I-R-542, CR Brasimone, 22 July 2022
12. N. Forgione, D. Martelli, G. Barone, F. Giannetti, P. Lorusso, T. Hollands, A. Papukchiev, M. Polidori, A. Cervone, I. Di Piazza, "Post-test simulations for the NACIE-UP benchmark by STH codes", *Nuclear Engineering and Design*, Volume **353**, November 2019, 110279
13. Handbook on lead-bismuth eutectic alloy and lead properties, material compatibility, thermal-hydraulics and technologies. OECD/NEA, 2015. https://inis.iaea.org/collection/NCLCollectionStore/_Public/46/133/46133907.pdf
14. D. Martelli, Ranieri Marinari, G. Barone, I. Di Piazza, M. Tarantino, CFD thermo-hydraulic analysis of the CIRCE fuel bundle, Ann. Nucl. Energy 103:294-305 (2017). https://doi.org/10.1016/j.anucene.2017.01.031
15. P. Cioli Puviani, I. Di Piazza, R. Marinari, R. Zanino, M. Tarantino, "Multiscale Thermal-Hydraulic Analysis of the ATHENA Core Simulator", ICONE29-93457, V008T08A064, 23 November 2022. https://doi.org/10.1115/ICONE29-93457
16. I. E. Idelchik, "Handbook of hydraulic Resistance", 3rd edition, *Jaico Publishing House* (2003)
17. S.K. Chen, R. Petroski, N.E. Todreas, "Numerical implementation of the Cheng and Todreas correlation for wire wrapped bundle friction factors-desirable improvements in the transition flow region", *Nucl. Eng. Des.,* **263**, pp. 406-410 (2013). https://doi.org/10.1016/j.nucengdes.2013.06.012
18. S.K Cheng adnd N.E. Todreas, "Hydrodynamic models and correlations for bare and wire-wrapped hexagonal rod bundles — Bundle friction factors, subchannel friction factors and mixing parameters", *Nucl. Eng. Des.*, **92**(2), pp. 227-251 (1986), https://doi.org/10.1016/0029-5493(86)90249-9
19. Information System Laboratories, "RELAP5/Mod3.3 code manual volume I: code structure, system models, and solution methods", July 2003